J. Biomed. Eng. Res.
Vol. 22, No. 5, 459-467, 2001

A New Experimental Error Reduction Method for Three-Dimensional Human Motion Analysis

Joung Hwan Mun

The Department of Biomedical Engineering, The Uiversity of Iowa, Iowa City, Iowa, 52242, U. S. A.

(Received November 17, 2000. Accepted October 8, 2001)

요 약 : Average Coordinate Reference System (ACRS) 방법은 인체 보행 분석 시 발생하는 실험오차를 줄이기 위해서 개발되었다. 실험적으로 측정되어지는 운동학 데이터가 인체 모델링 분석을 수행하기 위해서 사용되어지며, 그 모델의 정확성은 그 측정된 데이터에 직접적인 연관 관계가 있다. 그러나, 인체가 보행하는 동안에 피부의 움직임과 골격구조의 변형이 발생하고 또한 운동 분석 실험장비 자체가 가지고 있는 여러 가지의 한계 때문에, 그 실험 데이터에 정확도는 의문시되어 진다.
개발된 ACRS 방법은, 인체 운동분석을 수행하는 여러 종류의 시스템에 적용할 수 있는데, 본 연구에서는 ACRS 방법을 광학적으로 추적이 되는 표적을 인체의 각 세그멘트에 붙인 시스템에 적용하였다. ACRS 방법에서는, 각 세그멘트에 붙어있는 각각의 표적들이 독립적으로 그 세그멘트 안에서 국부좌표계의 원점으로 취급되어질 수 있다. 실험 과정에서 발생하는 본래부터의 오차 때문에, 각 원점에서 계산된 Euler angle은 서로 상이한 값을 갖는다. 실험 초기에 측정한 보정 세그멘트 기준 프레임의 지식을 이용하면, 각 표적 위치에서 계산된 Euler angles들의 평균값을 계산할 수 있고, 그 평균값은 피부의 확장과 회전의 영향을 최소화한 값이다. 운동분석에 일반적으로 적용되는 Euler angle 방법과 개발된 ACRS 방법을 비교하여 보면, ACRS 방법을 사용하였을 때 오차가 줄어들었다. 만약에, 보행 실험 데이터에 오차가 존재하지 않는다면, 절대좌표계를 사용한 무릎 관절의 분리와 관통된 거리는 일회 보행구간 동안에 제로가 될 것으로 생각된다. 일반적으로 적용되는 Euler angle 방법을 적용하였을 때, 분리와 관통된 거리는 약 18 mm 까지 분포가 되었고, 개발된 ACRS 방법을 사용하였을 시에는 약 12 mm 까지 분포가 되었다.

Abstract : The Average Coordinate Reference System (ACRS) method is developed to reduce experimental errors in human locomotion analysis. Experimentally measured kinematic data is used to conduct analysis in human modeling, and the model accuracy is directly related to the accuracy of the data. However, the accuracy is questionable due to skin movement, deformation of skeletal structure while in motion and limitations of commercial motion analysis system.
In this study, the ACRS method is applied to an optically-tracked segment marker system, although it can be applied to many of the others as well. In the ACRS method, each marker can be treated independently, as the origin of a local coordinate system for its body segment. Errors, inherent in the experimental process, result in different values for the recovered Euler angles at each origin. By employing knowledge of an initial, calibrated segment reference frame, the Euler angles at each marker location can be averaged, minimizing the effect of the skin extension and rotation. Using the developed ACRS methodology the error is reduced when compared to the general Euler angle method commonly applied in motion analysis. If there is no error exist in the experimental gait data, the separation and penetration distance of the femoraltibial joint using absolute coordinate system is supposed to be zero during one gait cycle. The separation and penetration distance was ranged up to 18 mm using general Euler angle method and 12 mm using the developed ACRS.
Key words : Gait analysis, Human motion, Joint coordinate, Knee joint, Biomechanics

INTRODUCTION

In clinical gait analysis, anatomical skin markers are generally employed as a tool to assess a patient's joint function and motion capability during pre- or post-rehabilitation [1-10]. In the most widely applied method, three markers are used for each body segment, with motion analysis hardware and software reducing the marker data to body segment location and orientation [1-5,11]. In the gait analysis experiment it is impossible to achieve error free position kinematics data because of skin movement, skeletal deformation and equipment errors [1-10]. In order to improve the accuracy of the motion experimental data, both experimental methods [5] and numerical methods [6,12] have reported in the previous studies.

In clinical human motion analysis, a general methodology for the kinematic data recovery is to use Euler angle orientation coordinates, Projected angle orientation coordinates or Helical angle orientation coordinates [2-3, 13-15]. In this study, the Euler angle method is used, so the

<속보논문>
통신저자 : Joung Hwan Mun, Ph. D, The Department of Biomedical Engineering
The College of Engineering
The University of Iowa Iowa City, Iowa, 52242, U. S. A.
Tel. 319-339-4234, Fax. 319-335-5631
E-mail. jmun@engineering.uiowa.edu

position and orientation of a body segment can be defined by the body-fixed local coordinates, $x' - y' - z'$, and three orientation coordinates which define the orientation of the body-fixed local coordinates relative to the global reference frame. An advantage of using the Euler angle method in human locomotion analysis is the capability of the complete three-dimensional motion representation using six parameters for each body segment. A disadvantage of the Euler angle method is that the values of the recovered orientation depend on the sequence of the three specific rotations [16]. The sequence of rotations used to define the final orientation of the coordinate system is to some extent arbitrary. A total of twelve conventions is possible using Euler angles in a right-hand coordinate system. The particular sequence of rotations used in this study is known as the *x convention*, while the angle coordinates resulting from the *xyz convention* are more commonly known as the Bryant angles [17].

Averaging techniques have frequently been used to recover better estimates of body segment orientation. These techniques involve averaging either the Euler-Bryant angles, or averaging of test trials. Orientation recovery, using Euler angle methods, depends on the sequence of the three rotations. Given three non-collinear anatomical markers, there exist six possible Euler angle rotational sequence permutations, $R_xR_yR_z$, $R_xR_zR_y$, $R_yR_xR_z$, $R_yR_zR_x$, $R_zR_xR_y$, and $R_zR_yR_x$, where R_i defines a given rotational axis. Panjabi et al. [11] *averaged* the results of these six possible permutations. This method has a theoretical problem since the values of the Euler angle rotations are dependent upon the sequence in which they were determined and the six Euler angle sequence permutations should not be directly added or averaged. In a different averaging technique, Kadaba et al. [4] performed a gait experiment using forty subjects three times on three different test days. By *averaging* several experimental data sets from a single subject, with respect to one gait cycle, he attempted to reduce errors in the motion analysis. Thus, a total of nine data sets for a particular subject were *averaged* with respect to normalized gait cycle length, irrespective of the actual stride distance or walking speed.

Another averaging technique, the Joint Averaging Coordinate System (JACS) technique, was suggested by Mun [2]. Even though rigid body assumptions are normally employed for kinematic and kinetic analysis in the biomechanics field, real experimental human motion data reflects deformable body motions. The JACS concept was developed based on this fact.

The object of this research is to propose a new error reduction method, the Averaged Coordinate Reference System (ACRS), which can be applicable directly in human motion analysis without any extra cost to existing motion analysis system. In this study, the ACRS method is applied to an optically-tracked segment marker system using Euler angle transformation recovery method, although it can be applied to many of the others as well. In the ACRS method, each marker mounted on the skin is treated independently, as the origin of a local coordinate system for its body segment. Errors, inherent in the experimental process, result in different values for the recovered Euler angles at each origin. By employing knowledge of an initial, calibrated segment reference frame, the Euler angle at each marker location can be averaged, minimizing the effect of the skin extension and rotation, and other experimental errors. In order to provide better communication with clinical personnel, results of the gait analysis are presented using clinically meaningful terminology [14], such as flexion/extension, adduction/abduction and external/internal rotation.

ANALYSIS

Euler angles are the most common parameters used to describe the spatial orientation of a body. Using the *x convention*, the angular orientation of a body fixed local coordinate system, $x' - y' - x'$, with respect to global $x - y - z$ coordinate system can be obtained by the three successive rotations such as Ψ, θ, and ϕ by the rotation order of $z - x' - z''$ axis, respectively as shown in Figure 1.

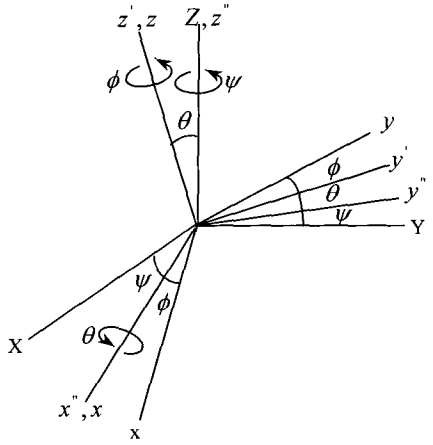

Fig. 1. The Rotations Defining the Euler Angles

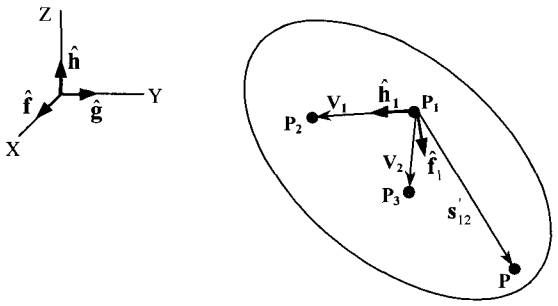

Fig. 2. The Configuration of the Three Marker System

The Euler angles for each body segment can be obtained from the experimental position marker data as shown in Figure 2. Here, P_1, P_2 and P_3 represent the markers attached to a body segment during the experiment. Each marker can be independently treated as the origin of a local coordinate system. For example, starting with marker P_1, a body coordinate frame can be determined, whose orientation to the global reference frame is given by the transformation matrix, A_1. This transformation can be expressed as

$$A_1 = \begin{bmatrix} a_{11} & a_{12} & a_{13} \\ a_{21} & a_{22} & a_{23} \\ a_{31} & a_{32} & a_{33} \end{bmatrix} = [\ \hat{f}_1\ \ \hat{g}_1\ \ \hat{h}_1] \tag{1}$$

where the columns of are the orthogonal unit vectors, $\hat{f}_1$, $\hat{g}_1$ and $\hat{h}_1$. These unit vectors can be determined from the marker points, P_1, P_2 and P_3, by first creating the vectors, v_1 and v_2, which point from marker location P_1 to markers P_2 and P_3 as

$$v_1 = P_2 - P_1 \tag{2}$$

$$v_2 = P_3 - P_1 \tag{3}$$

So that $\hat{f}_1$, $\hat{g}_1$ and $\hat{h}_1$ can be expressed using basic vector operations as follows.

$$\hat{\mathbf{h}}_1 = \frac{\mathbf{v}_1}{\|\mathbf{v}_1\|} \tag{4}$$

$$\hat{\mathbf{f}}_1 = \frac{\mathbf{v}_1 \times \mathbf{v}_2}{\|\mathbf{v}_1 \times \mathbf{v}_2\|} \tag{5}$$

$$\hat{\mathbf{g}}_1 = \hat{\mathbf{h}}_1 \times \hat{\mathbf{f}}_1 \tag{6}$$

By redefining the vectors v_1 and v_2 in Eqs. (2) and (3), to use points P_2 and P_3 as origins, equivalent transformation matrices can be formed from these marker locations as well.

More generally, using the *x convention* for determining Euler angles, the structure of the transformation matrix, , can be equivalently expressed as

$$\mathbf{A}_i = \begin{bmatrix} \cos\psi\cos\phi - \sin\psi\cos\theta\sin\phi & -\cos\psi\sin\phi - \sin\psi\cos\theta\cos\phi & \sin\psi\sin\theta \\ \sin\psi\cos\phi + \cos\psi\cos\theta\sin\phi & -\sin\psi\sin\phi + \cos\psi\cos\theta\cos\phi & -\cos\psi\sin\theta \\ \sin\theta\sin\phi & \sin\theta\cos\phi & \cos\theta \end{bmatrix} \tag{7}$$

Thus, the Euler angles can be determined using the folloing equations.

$$\psi = -\tan^{-1}\left(\frac{\sin\psi}{-\cos\psi}\right) = -\tan^{-1}\left(\frac{a_{13}}{a_{23}}\right) \tag{8}$$

$$\theta = \cos^{-1}(a_{33}) \tag{9}$$

$$\phi = \tan^{-1}\left(\frac{\sin\phi}{\cos\phi}\right) = \tan^{-1}\left(\frac{a_{31}}{a_{32}}\right) \tag{10}$$

AVERAGED COORDINATE REFERENCE SYSTEM (ACRS)

If no experimental error exists, the resulting inverse kinematic recovery of the Euler angles is not affected by a number of markers because the constant distance vector separating each marker at the standing calibration stage is unchanged during motion. However, skin extension and skin rotation exist during subject locomotion, causing localized changes in each marker's location. These and other experimental errors produce different results for the recovered Euler angles at each origin. Thus, three different results can be determined from just three markers since each marker can be a local origin and the effect of the skin extension and skin rotation is different from the others as shown in Figure 3. A_{12} and A_{13} are constant transformation matrices from the origin P_2 and P_3 to the origin P_1, respectively. These transformation matrices are determined during calibration, with the subject at a standing position.

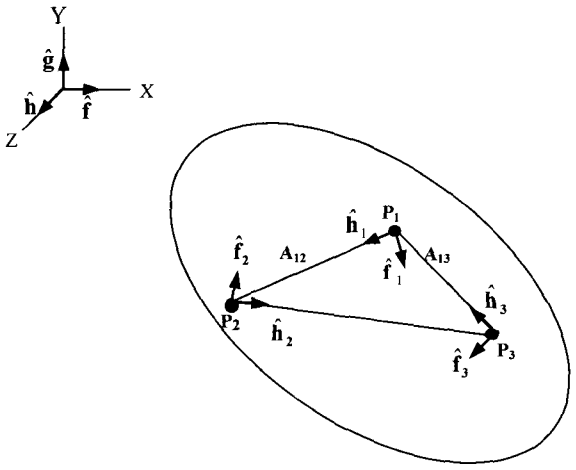

Fig. 3. Configuration of the ACRS

$$\mathbf{A}_{12} = \mathbf{A}_2^{-1}\mathbf{A}_1 \tag{11}$$

$$\mathbf{A}_{13} = \mathbf{A}_3^{-1}\mathbf{A}_1 \tag{12}$$

Thus, the relationship of A1, A2, and A3 can be written as

$$\mathbf{A}_1 = \mathbf{A}_2\mathbf{A}_{12} = \mathbf{A}_3\mathbf{A}_{13} \tag{13}$$

In the Eq. (13) A_1, A_2, and A_3 are the transformation matrices from the each origin's local coordinate system to the global coordinate system while in motion. However, if errors exist for the marker position data, then,

$$\mathbf{A}_1 \neq \mathbf{A}_2\mathbf{A}_{12} \neq \mathbf{A}_3\mathbf{A}_{13} \tag{14}$$

Using the relationship of Equation (14), transformations from each of the three reference frame combinations for three markers system can be transformed to the segment's base reference frame. Then applying Equations (8)-(10), the Euler angles for each of the three permutations can be determined. The Euler angles are then averaged using the equations

$$\psi^{ave} = \frac{1}{N}\sum^{N}\psi^i \tag{15}$$

$$\theta^{ave} = \frac{1}{N}\sum^{N}\theta^i \tag{16}$$

$$\phi^{ave} = \frac{1}{N}\sum^{N}\phi^i \tag{17}$$

In the Eqs. (15)-(17), N is three for three skin marker system, and twelve and thirty for four and five skin marker system, respectively, excluding mirror image permutations. The averaged transformation, A_{ACRS}, representing the ACRS local to global transformation, is then calculated by using the averaged Euler angle in Equation (7).

In order to verify the proposed ACRS method, a simple 3-D knee joint contact model was developed, employing an absolute coordinate system. In the previous publication [2], the computational modeling and contact detection technique to compute the separation and penetration distance in the femoraltibial joint has been described in detail. A brief description of the model is included here in the interest of continuity. The model is a 6 DOF knee joint represented by two spheres considering sliding and rolling as shown in Figure 4. The lateral and medical condyle are assumed spherical having fixed radii of 20.4 mm and 19.9 mm, respectively [19]. The tibial articulating surface was assumed to be flat [20]. In Figure 4, the vector position of the center of two spheres P_{11} and P_{12} can be expressed in terms of the global Cartesian reference coordinate system as

$$\mathbf{P}_{11} = \mathbf{r}_1 + \mathbf{A}_1\mathbf{s}'_{p11} \tag{18}$$

$$\mathbf{P}_{12} = \mathbf{r}_1 + \mathbf{A}_1\mathbf{s}'_{p12} \tag{19}$$

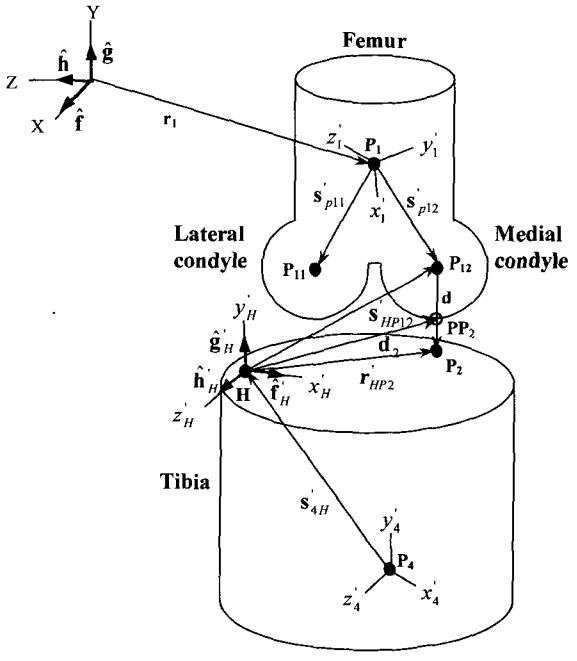

Fig. 4. The Configuration of the Knee Joint Contact Model

r_1 is the vector from the origin of the global laboratory reference to the local origin of femur segment and A_1 is the transformation matrix from the local coordinate system of the femur to the global coordinated system during the motion. The constant local vectors s'_{p11} and s'_{p12} are calculated from the calibration stage data as

$$\mathbf{s}'_{p11} = \mathbf{A}_{1s}^{-1}(\mathbf{r}_1 - \mathbf{P}_{11}) \tag{20}$$

$$\mathbf{s}'_{p12} = \mathbf{A}_{1s}^{-1}(\mathbf{r}_1 - \mathbf{P}_{12}) \tag{21}$$

where $\mathbf{A}_{1s}^{-1}$ is the inverse matrix of the transformation matrix A_{1s} calculated at the calibration data set.

In the development of the following computational model, the medial condyle and tibia plateau will be considered as the example. Development of the lateral condyle side equations is the same as the medial condyle case. An arbitrary point H is placed on the tibia surface can be expressed as

$$\mathbf{H} = \mathbf{r}_4 + \mathbf{A}_2\mathbf{s}'_{4H} \tag{22}$$

where r_4 is the vector from the origin of the global coordinate system to the local origin of tibia segment and s'_{4H} is a constant vector given in the segment's local coordinate system. This vector can be calculated at the calibration stage and characterized by

$$\mathbf{s}'_{4H} = \mathbf{A}_{2s}^{-1}(\mathbf{r}_4 - \mathbf{H}) \tag{23}$$

where is the inverse matrix of the transformation matrix A_{2s}^{-1} calculated at the calibration position.

The calculation procedure of the contact point of the medial condyle on the tibia plateau, P_2, follows. The contact point P_2 can be expressed in terms of global Cartesian coordinate system as

$$\mathbf{P}_2 = \mathbf{H} + \mathbf{A}_2\mathbf{C}'_o\begin{Bmatrix} a \\ 0 \\ c \end{Bmatrix} \tag{24}$$

$$\mathbf{C}'_o = \mathbf{A}_{2s}^{-1} \tag{25}$$

where, is the constant transformation matrix between marker number 4 and position H at the standing calibration stage. The scalar values, a and c, are the distance from position H to the contact point P_2 in terms of local coordinate system of x'_H, and z'_H. The geometric compatibility condition is that the vector d has to be perpendicular to the unit vectors $\hat{\mathbf{f}}$ and $\hat{\mathbf{g}}$ to satisfy the contact condition. Thus, the dot product equations can be written as

$$\mathbf{d} \bullet \hat{\mathbf{f}} = \mathbf{d} \bullet \mathbf{A}_2\mathbf{C}'_o\hat{\mathbf{f}}'_H = 0 \tag{26}$$

$$\mathbf{d} \bullet \hat{\mathbf{h}} = \mathbf{d} \bullet \mathbf{A}_2\mathbf{C}'_o\hat{\mathbf{h}}'_H = 0 \tag{27}$$

And, the scalar distances a and c can be determined as

$$a = \hat{\mathbf{f}}(\mathbf{P}_1 - \mathbf{H}) = \hat{\mathbf{f}}^T\mathbf{A}_2\mathbf{C}'_o\begin{Bmatrix} a \\ 0 \\ c \end{Bmatrix} = \begin{Bmatrix} 1 \\ 0 \\ 0 \end{Bmatrix}^T \mathbf{C}_o^T\mathbf{A}_2^T\mathbf{A}_2\mathbf{C}'_o\begin{Bmatrix} a \\ 0 \\ c \end{Bmatrix} \tag{28}$$

$$c = \hat{\mathbf{h}}(\mathbf{P}_1 - \mathbf{H}) = \hat{\mathbf{h}}^T\mathbf{A}_2\mathbf{C}'_o\begin{Bmatrix} a \\ 0 \\ c \end{Bmatrix} = \begin{Bmatrix} 0 \\ 0 \\ 1 \end{Bmatrix}^T \mathbf{C}'^T_o\mathbf{A}_2^T\mathbf{A}_2\mathbf{C}'_o\begin{Bmatrix} a \\ 0 \\ c \end{Bmatrix} \tag{29}$$

Since separation and penetration is allowed in the computational knee joint model, there exist two contact points for medial condyle such as P_2 and PP_2 while in motion.

$$\text{distance} = \hat{\mathbf{g}}'^T_H\mathbf{d}_2 \tag{30}$$

$$\hat{\mathbf{g}}'_H = \hat{\mathbf{h}}'_H \times \hat{\mathbf{f}}'_H \tag{31}$$

In the experimental data recovery, the separation and penetration distance of knee joint is supposed to be zero during one gait cycle. However, in experimental clinical gait analysis, random and systematic errors caused by skin movement, skeletal deformation and equipment error leads separation and penetration at the knee joint during one gait cycle. Thus, the separation and penetration distance using general Euler Angle technique (EA) and ACRS were calculated and compared.

EXPERIMENTS

Experimental gait data from a normal, healthy male (29 years old, 76 Kg, and height 174 cm) with a free walking speed of 1.4 m/sec was used as input for the inverse

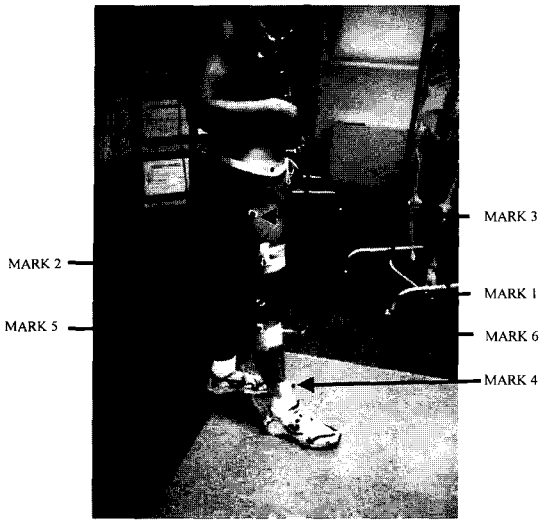

Fig. 5. The Anatomical Marker System

kinematic analysis. As shown in Figure 5, the thigh segment was tracked using a total of three IREDs, placed along the lateral thigh, spaced at approximately 15 cm intervals with the middle IRED on a 5.5 cm extension. The shank segment was tracked using three IREDs paced along the tibia separated by approximately 15 cm with the middle IRED mounted on a 7 cm extension. The IREDs were tracked using an Optotrak motion analysis system (model 3020, Northern Digital, Waterloo, Ontario) at 60 Hz. The subject walked along a 30m walkway which contained a 3 m by 2 m data collection volume with an estimated accuracy of less than 1mm in all directions. Marker data were filtered at 6 Hz using a 4^{th} order Butterworth filter. In addition, an aluminum clamping device (185 g) leading minimal skin movement error during gait [18] was positioned over the femoral condyles with a 10 cm rod extending laterally with one IRED (marker P). In the analysis, the fourth marker (marker P) on the thigh segment was used to perform the experimental validation and to verify the effectiveness of the ACRS method.

RESULTS

As shown previously in Figure 2, the global position of an arbitrary point P can be expressed from each of the known marker positions, P_1, P_2, or P_3, as one of the three Eqs (32), (33) or (34),

$$\mathbf{r}^P = \mathbf{r}_1 + \mathbf{A}_1\mathbf{s}'_{1P} \tag{32}$$

$$\mathbf{r}^P = \mathbf{r}_2 + \mathbf{A}_2\mathbf{s}'_{2P} \tag{33}$$

$$\mathbf{r}^P = \mathbf{r}_3 + \mathbf{A}_3\mathbf{s}'_{3P} \tag{34}$$

where r_1, r_2 and r_3 are vectors from the global coordinate reference frame to the each three different local coordinate reference frames, while A_1, A_2 and A_3 are the respective transformation matrices from the local coordinate systems to the global coordinate system while in motion, and S'_{1P}, S'_{2P} and S'_{3P} are constant vectors defined with respect to the segment's local coordinate system.

One gait cycle of the displacement motion from the experiment is shown in Figures 6, 7, and 8, for the global x, y, and z directions, respectively. The magnitude of the data ranged about 1600 mm. for the sagittal plane motion (x direction), 80 mm. for the frontal plane motion (y direction) and 40 mm. for the transverse plane motion (z direction). Thus, comparative results are more sensitively affected for the frontal and transverse plane motion than that of the sagittal plane motion, due to the relative magnitude of the data.

In Figure 6, the labels P_x, EA_x and ACRS_x represent the experimentally measured sagittal plane displacement of the arbitrary point P (Marker P) on the

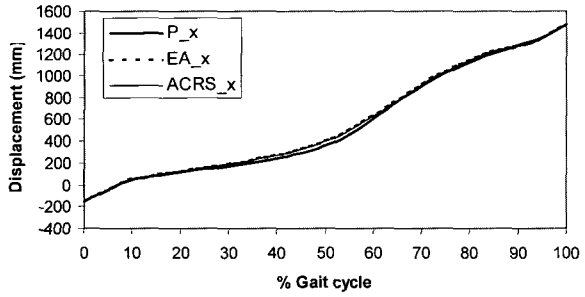

Fig. 6. Comparison of the Sagittal Plane Motion for Point P

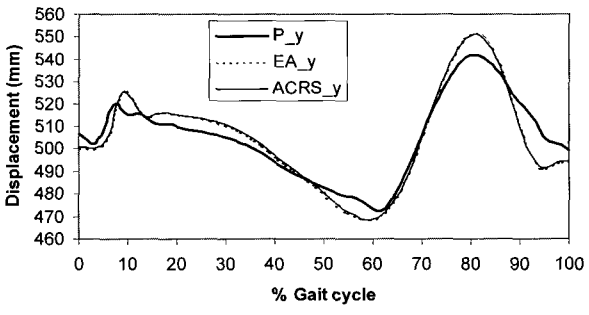

Fig. 7. Comparison of the Frontal Plane Motion for Point P

thigh segment, the calculated displacement of the point P using Euler angles recovered from the three-marker set, and the calculated displacement of the point P using the ACRS technique with the same three-marker set, respectively. The ACRS method compares favorably with the general Euler angle technique when tracking the motion of the point P.

In Figure 7, the labels P_y, EA_y and ACRS_y represent the experimentally measured frontal plane displacement of the arbitrary point P (Marker P), the calculated displacement of the point P using the general Euler angle technique, and calculated displacement of the point P using the ACRS technique, respectively. Results of the ACRS method show little difference to that of the general Euler angle technique, and both methods differ from the experimentally measured value over similar portions of the gait cycle. The lack of improved results using the ACRS technique is likely due to the measured errors in this direction being systematic and not random. Statistical averaging will only affect random errors.

In Figure 8, the labels P_z, EA_z and ACRS_z represent the experimentally measured transverse plane displacement of the arbitrary point P (Marker P), the calculated displacement of the point P using the general Euler angle technique and the calculated displacement of the point P using the ACRS technique, respectively. Results of the ACRS method show closer agreement with the experimentally measured values than the results of the general Euler angle technique. Unlike the frontal plane results, shown previously in Figure 7, the results shown in Figure 8 exhibit both systematic and random errors, such that the ACRS technique can reduce but not eliminate discrepancies with the experimental data.

The relative motions between the femur and tibia segments using Grood and Suntay's anatomical coordinate [14] in terms of flexion/extension, adduction/abduction and external/internal rotations using the standard three skin marker system are shown in Figures 9, 10 and 11, respectively. The plots in the dot line such as A_123, A_231 and A_312 show the individual curves for each marker combination, while the solid bold line shows the value as determined by the ACRS method. For example, A_123 represents that the skin maker P1 as shown in Figure 2 is taken as the origin of the local reference frame. A_231 and A_312 represent that the marker P_2 and P_3 are used as the origin of the local reference coordinate system, respectively.

From the individual curves for each marker combination, the difference between the maximum and minimum flexion/extension angle is about eight degrees, which occurs during the stance phase, at 40% of the gait cycle. The maximum difference for adduction/abduction angle occurred at the same point as the flexion/extension, with the difference being approximately four degrees. The maximum difference for the internal/external rotation angle being about fourteen degrees occurred during swing phase, at 90% of the gait cycle. Interestingly the third recovered angle, internal/external rotation, has a relatively high value of standard deviation compared to flexion/extension and adduction/abduction rotation angles through the entire gait cycle. This implies the least confidence in the value of the recovered external/internal rotation angle, as shown by other researchers [6,14-15]. Additionally, the relatively large differences between knee joint rotation angles recovered through the use of different marker combinations lends justification to the ACRS technique, which averages the differences, as opposed to the use of a single marker combination.

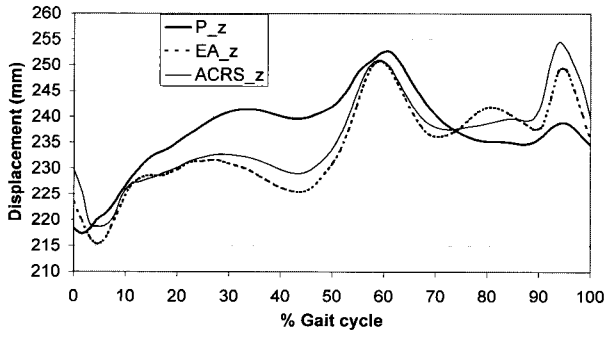

Fig. 8. Comparison of the Transverse Plane Motion for Point P

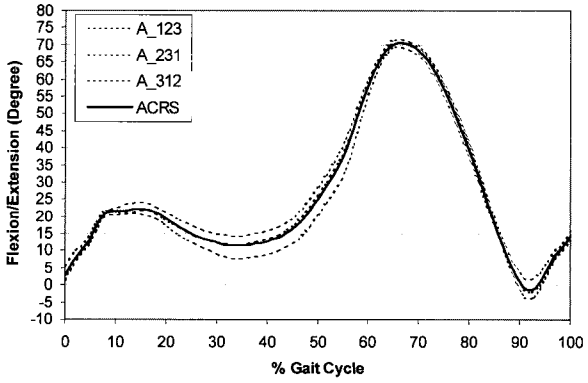

Fig. 9. Relative Flexion/Extension Angle between Femur and Tibia Segment during One Gait Cycle

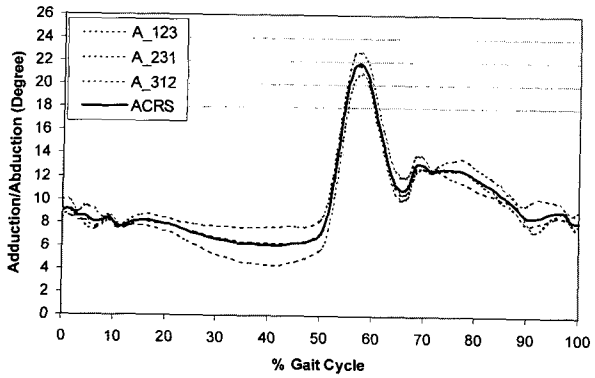

Fig. 10. Relative Adduction/Abduction Angle between Femur and Tibia Segment during One Gait Cycle

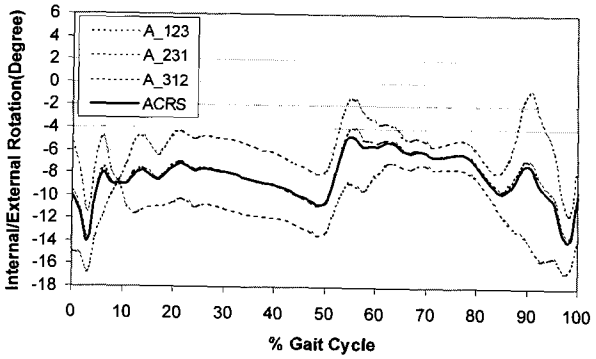

Fig. 11. Relative Internal/External Angle between Femur and Tibia Segment during One Gait Cycle

(A) Medial Side

(B) Lateral Side

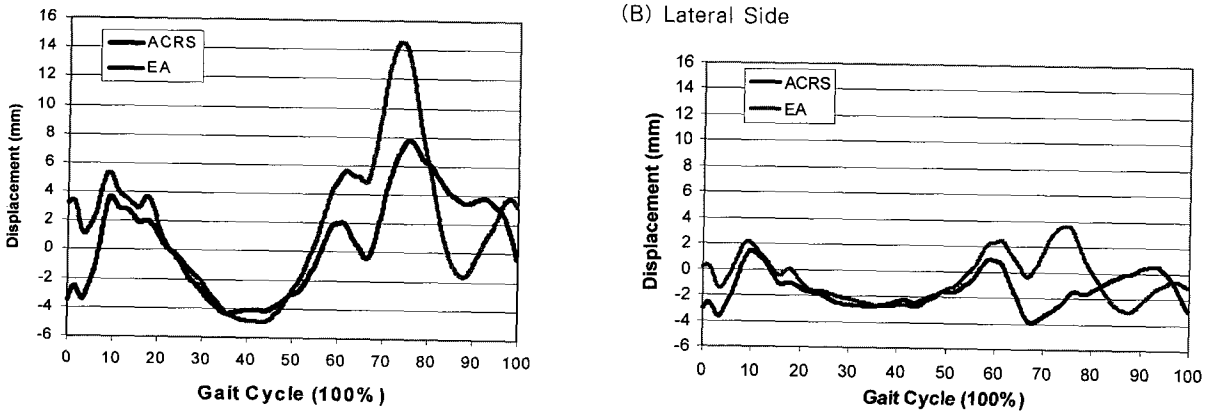

Fig. 12. Separation and Penetration Distance Plot Using General Euler Angle Technique (EA) and ACRS

The separation and penetration distance of the contact point at medial condyle and tibial articulating surface during one gait cycle was ranged about 18 mm for the general Euler angle technique and 12 mm for the proposed ACRS technique. The separation and penetration distance at the lateral side was ranged about 5 mm for SE and ACRS as shown in Figure 12. The absolute averaged value (±S.D) of the separation and penetration during one gait cycle at the medial side is 3.0 (±1.8) mm and 4.0 (±3.2) mm for ACRS and general Euler angle (SE) technique, respectively, while lateral side ranged 1.6 (1.0) mm for both ACRS and SE technique. In addition, the maximum absolute value of the separation/penetration during swing phase of the gait cycle at the medial side is about 12 mm and 19 mm for ACRS and SE technique, respectively.

CONCLUSIONS

This study has presented a statistically based method for reducing errors associated with recovery of orientation coordinates from anatomical landmark marker data. The Averaged Coordinate Reference System (ACRS) technique can be applied whenever multiple marker data sets are employed to determine body segment orientation. The ACRS technique is independent of the coordinate system used. In this study, the conventional Euler angle system was applied, however any coordinate system could have been used.

The ACRS method is an analytical approach to enhance the clinical interpretation of movement data. The ACRS technique statistically averages random errors due to skin movement and data acquisition. Given three anatomical markers, three values for each of the Euler angles can be averaged. However, if more markers are included on a body segment, many more combinations of the Euler angles are possible. For instance, a four-marker system will generate twelve unique sets of Euler angles, while a five-marker system results in thirty unique sets excluding mirror-image combinations. Finite statistics

shows that predicted values for body segment orientation will tend toward the true values as the number of averaged values increases. This assumes that errors in the experimental data are randomly distributed, and follow a normal distribution. As seen from the results, not all errors acquired in human motion analysis are random. Many are systematic. Statistical methods like the ACRS can be applied in conjunction with other techniques, such as skin movement compensation [8] which addresses systematic errors in marker location, to lead to improved assessment of human motion.

Acknowledgements

The author would like to thank Professor Kwan Rim in the Department of Biomedical Engineering, Professor Jeffrey Freeman in the Department of Mechanical Engineering and Professor John Yack of the Gait Laboratory in the Department of Physical Therapy at the University of Iowa for valuable discussions.

REFERENCES

1. J. Fuller, L.J. Liu, M. Liu, C Murphy and R.W. Mann, "*A comparison of lower-extremity skeletal kinematics measured using skin- and pin-mounted markers*", Human Movement Science, Vol. 16, pp. 219-242, 1997
2. J.H. Mun: Human gait analysis using multi-body dynamics and contact modeling, Ph. D. Thesis, The University of Iowa, Iowa City, Iowa, 1998
3. J.H. Mun, J.S. Freeman, and K. Rim, "*A statistical data reduction method for application in human knee joint during gait*", Gait & Posture, Vol. 9 (Suppl. 1), pp. S53, 1999
4. M.P. Kadaba, H.K. Ramakrishan and M.E. Wootten, "*Measurement of lower extremity kinematics during level walking*", J. of Orthopedic Research, Vol. 12, No. 6, pp. 769-779, 1994
5. A. Cappozzo, "*Three-dimensional analysis of human walking : Experimental methods and associated artifacts*", Human Movement Science, Vol. 10, pp. 589-602 1991
6. L. Cheze, B.J. Fregly and J. Dimnet, "*A solidification procedure to facilitate kinematic analysis based on video system data*", J. of Biomechanics, Vol. 28, pp. 879-884, 1995
7. A. Cappello, A. Cappozzo, P.F.L. Palombara, L. Lucchetti, and A. Leardini, "*Multiple anatomical landmark calibration for optimal bone pose estimation*", Human Movement Science, Vol. 16, pp. 259-274, 1997
8. L. Lucchetti, A. Cappozzo, A. Cappello, and U.D. Croce, "*Skin movement artefact assessment and compensation in the estimation of knee-joint kinematics*", J. of Biomechanics, Vol. 31, pp. 977-984, 1998
9. C. Reinschmidt, A.J. van den Bogert, B.M. Nigg, A. Lundberg, and N. Murphy, "*Effect of skin movement on the analysis of skeletal knee joint motion during running*", J. of Biomechanics, Vol. 30, pp. 729-732, 1997
10. T. Teager and J.H. Somerset, "*Investigation of the error caused by femur movement attendant to an in vivo study of human knees*", J. of Biomechanics, Vol. 9, pp. 659-661, 1976
11. M.M. Panjabi, O. Takeori, J.J. Crisco III, J. Dvorak, and D. Grob, "*Posture affects motion coupling patterns of the upper cervical spine*", J. of Orthopaedic Research, Vol. 11, pp. 525-536, 1993
12. I. Soderkvist and P. Wedin, "*Determining the movements of the skeleton using well-configured markers*", J. of Biomechanics, Vol. 26, pp. 1473-1477, 1993
13. E.Y.S. Chao, "*Justification of triaxial goniometer for the measurement of joint rotation*", J. of Biomechanics, Vol. 13, pp. 989-1006,1980
14. E.S. Grood and W.J. Suntay, "*A joint coordinate system for the clinical description of three-dimensional motions : application to the knee*", J. of Biomechanical Engineering, Vol. 105, pp. 136-144, 1983
15. H.J. Woltring, "*Representation and calculation of 3-D joint movement*", Human Movement Science, Vol. 10, pp. 603-616, 1991
16. W. Skalli, F. Lavaste and J.L. Descrimes, "*Quantification of three-dimensional vertebral rotations in scoliosis : What are the true values?*", Spine, Vol. 20, pp. 546-553, 1995
17. P.E. Nikravesh: Computer-aided analysis of mechanical systems, Prentice-Hall Inc., Englewood cliffs, New Jersey, 1988
18. J.S. Houck: *Comparison of knee kinematics and kinetics of ACL deficient subjects performing straight-ahead and crossover-cutting activities, Ph. D. Thesis dissertation, The University of Iowa, Iowa City*, Iowa, 1999
19. H. Kurosawa, P.S. Walker, S. Abe, A. Grag and T. Hunter, "*Geometry and motion of the knee for implant and orthotic design*", J. of Biomechanics, Vol. 18, pp. 487-499, 1985
20. D.R. Wilson and J.J. O'Connor, "*A three-dimensional geometric model of the knee for the study of joint forces in gait*", Gait & Posture, Vol. 5, pp. 108-115, 1997